Aquifer mapping in Deep water Miocene sand using Extended Elastic Impedance Attributes -A case study from Mahanadi Basin

Ashish Kumar Singh, Indrajit Das, Tejpunj Jhaldiyal, Aramudi Ravi, Anurag Chaudhary*

Reliance Industries Limited, Mumbai (India)

Email:ashish.k.singh@ril.com

Keywords

Reservoir, Characterization, Aquifer, EEI, LR, SI, Vp/Vs, Density, Porosity

Summary

Characterization of brine sand is equally as important as characterization of hydrocarbon bearing sand for a development field. The development strategy such as well type and well placement are often influenced by aquifer size and behavior. Most of the times it is found that elastic properties of brine sand overlaps with that of background shale. However with the application of effective seismic inversion techniques, the characterization of brine sands could be achieved.

Post stack and Pre Stack seismic inversion are widely used to characterize the reservoir. Often, it has been observed that post stack inversion (acoustic impedance) is not always suitable to discriminate gas sands and brine sands due to its zero offset assumptions. This leads to use of more advanced pre stack inversion techniques like simultaneous inversion (SI) and Extended Elastic Impedance inversion (EEI). Simultaneous inversion (SI) effectively handles two term AVO equation better than three terms. Consequently, properties like density which correlate at higher angles is not very well captured by SI. EEI solves this problem very efficiently; it gives flexibility of wider range angles (+90 to -90), by substituting $\tan\chi$ for $\sin^2\theta$ in the two-term reflectivity equation (Whitcomb, 2002).

In the present study, extension of brine sand has been analyzed and mapped by density and porosity attributes generated using EEI approach. Further, these attributes are used to define the facies in the geocellular model. Dynamic modeling has been carried out to assess the impact of the brine sand on the field performance. This approach helped in optimizing the placement of development wells by mitigating the risk of early water influx thus adding confidence to the production performance prediction.

Introduction

The study area comprises of approximately 150 sq. km lies in offshore Mahanadi Basin, East coast of India. The geological settings are defined by channelized fan lobes, deposited on proximal part of the basin floor fan. The two wells A and B were drilled in the area. Well A encountered gross interval of 35 m gas sand, however 30 m brine sand was found in well B.The entrapment is envisaged to be stratigraphic in nature with good NTG sand reservoirs.

Wells A and B were drilled at a water depth of 512 m and 312 m respectively. The top of the gas reservoir was interpreted at depth 3642 m and GWC was established at depth 3677 m on the basis of well log and MDT data. Second well B was drilled to target the seismically and stratighaphically equivalent event of gas reservoir of well A, but it encountered the brine sand at depth 3720 m down dip (Figure-1). Sand quality of both the reservoirs is good, with grain size coarse to medium deposited as alternate sand/shale sequence. Average porosity of the reservoirs is in the range 15% to 20%.

The lateral as well as vertical variability of gas sand and brine sand are very well captured in seismic attributes and well data. Multiple approaches of inversion were used to characterize the extension of aquifer and gas sand. Starting from Post stack inversion to advanced EEI were attempted. Although P-impedance attribute effectively characterizes the gas sand, but it's not able to substantially delineate water sand. P-impedance attribute map covering both gas and brine sand is shown in Figure-2.Consequently, EEI has been carried out, with porosity and density as target log for generation of porosity and density attribute volumes. These attributes were utilized to capture the sand facies distribution in geocellular model. Aquifer is considered below the encountered GWC in well A.

Reservoir simulation was carried out to understand the impact of brine sand on the reservoir performance. Analytical aquifer model replicating the mapped brine sand helped to optimize the development strategy by indicating more suitable well locations based on water movement.

Aquifer mapping in Deep water Miocene sand using Extended Elastic Impedance Attributes -A case study from Mahanadi Basin

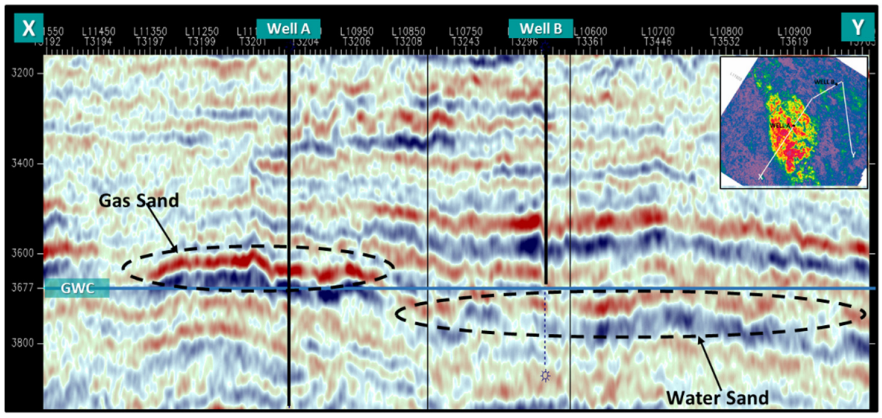

Figure-1 Seismic depth section showing Gas and Brine sand encountered at same stratigraphic level.

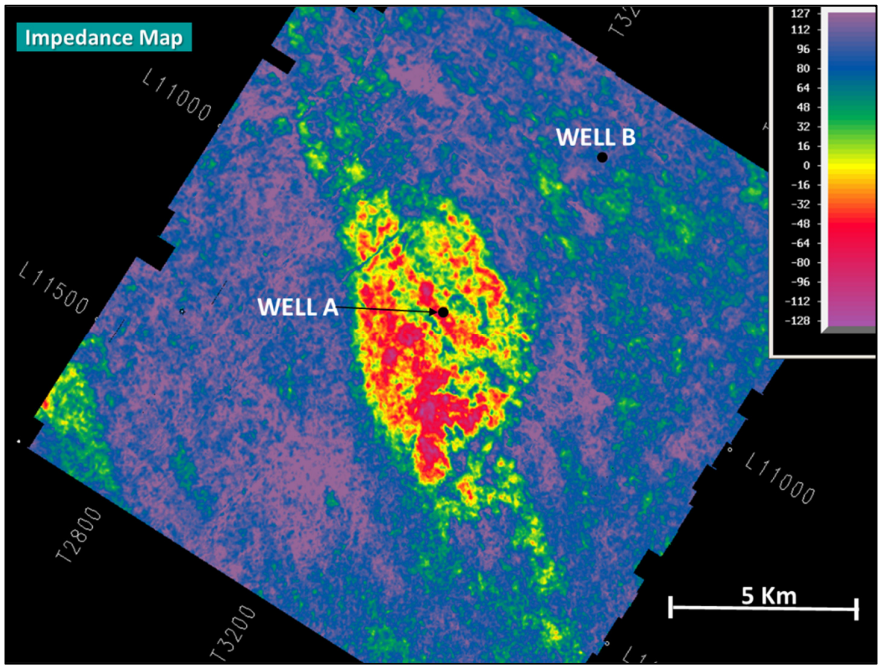

Figure-2 P-Impedance attribute map showing the effective delineation of Gas Sand in comparison to brine sand.

Rock physics analysis and EEI attributes Identification

A detailed rock physics analysis was carried out to find out most suitable acoustic/elastic property, which can be generated from EEI and used to identify gas and water sands away from well. In the P-impedance log, gas zone shows fair lowering, however high impedance response was observed for brine sand, thus limiting discrimination of reservoir sands using a single attribute cutoff in geo cellular model. Subsequently, Density, porosity, Vp/Vs and LR logs were analyzed. It was observed that reservoirs are slightly better defined in porosity and density compared to LR and Vp/Vs as shown in Figure-3. So, density and porosity were identified as EEI attributes and corresponding volumes were generated.

Aquifer mapping in Deep water Miocene sand using Extended Elastic Impedance Attributes -A case study from Mahanadi Basin

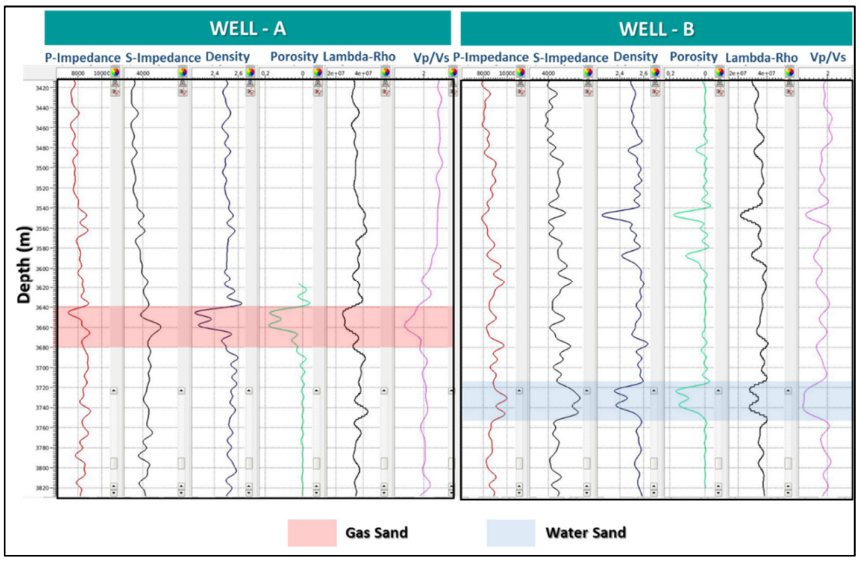

Figure-3 Well logs of Well A and Well B with High cut filter applied.

Seismic Data

Pre Stack Depth Migrated (PreSDM) processed Seismic data was used after data conditioning in the study. Utmost care was taken for AVO friendly processing through relative amplitude preservation having high signal to noise ratio. This in turn helped generating very stable intercept, gradient and angle stacks volumes, which was used in EEI inversion to generate robust property volumes for the reservoir sand discrimination from the background shale.

EEI Methodology

The analysis was performed on intercept, gradient and EEI logs in Jason's JGWTM and CGG Hampson Russel software. There are three basic steps involved in EEI inversion. First step was generation of log spectrum for the angle range -90 to +90° by using P-Sonic, S-Sonic and Density logs recorded at the well. In the second step, Chi angles for petro physical properties was determined .The seismic reflectivity volumes were generated using chi angles at which target petro physical properties had the maximum correlation. Finally, well to seismic tie, wavelet extraction and inversion were carried out on reflectivity volumes to obtain the property volumes in extended elastic impedance form.

The equation to compute extended elastic impedance at an angle of incidence θ, replacing $\sin^2\theta$ by $\tan\chi$ in two term linearized Zoeppritz equation (Whitcombe, 2002) is:

$$Rs = (A\cos\chi + B\sin\chi)$$

Equation written as EI equivalent

$$EEI(\chi) = (V_{p0} * \rho_0) * \left[\left(\frac{V_p}{V_{p0}}\right)^p * \left(\frac{V_s}{V_{s0}}\right)^q * \left(\frac{\rho}{\rho_0}\right)^r\right]$$

Here, $p=(\cos\chi + \sin\chi)$, $q=-8K\sin\chi$, $r=(\cos\chi - 4K\sin\chi)$

and $K = V_s^2/V_p^2$

Vp, Vs and ρ are the parameters as observed at the well and are available from standard log suite. Vp_0,Vs_0 and ρ_0 are the average value of these parameters over background shale region. Typically, for $\chi = 0$; EEI= [Vp*ρ] i.e. acoustic impedance. EEI spectrum logs were cross plotted against the target log (density and porosity) to determine the appropriate Chi angle which represents the target logs. Maximum correlation at chi angles 20^0 and 25^0 was observed for density and porosity as shown in Figure-4. EEI (20^0) and EEI (25^0) logs indicated good correlation with density and porosity logs Figure-5.

As the final step of work flow, reflectivity volumes were calculated at the chi angles 20^0 and 25^0 which represent the density and porosity. Therefore, both the reflectivity volumes were inverted using wavelets derived from calibration using both the logs EEI (20^0) and EEI (25^0) respectively. Inverted EEI volumes significantly delineated both the reservoirs from the back ground shale (Figure-6).

Aquifer mapping in Deep water Miocene sand using Extended Elastic Impedance Attributes -A case study from Mahanadi Basin

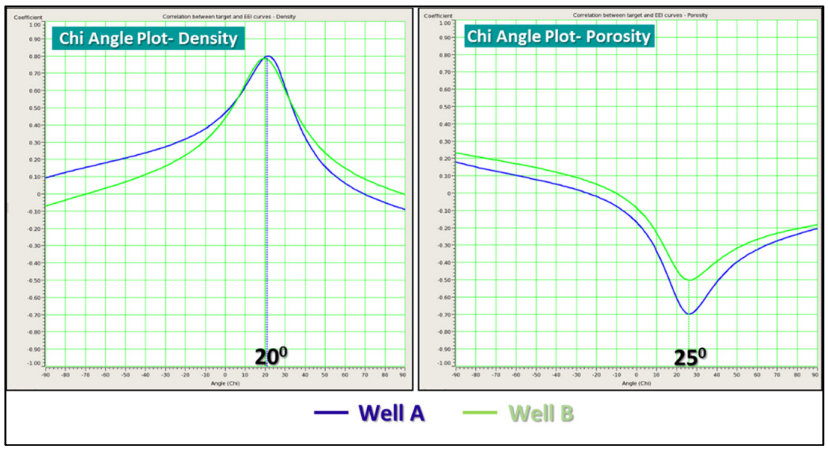

Figure-4 Chi Angle Analysis plot for Density and Porosity as target log.

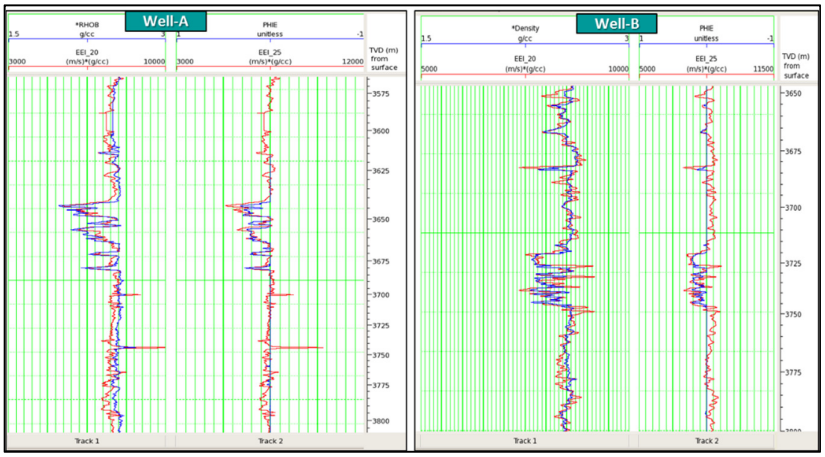

Figure-5 EEI (20) & EEI (25) logs overlain by Density and Porosity logs.

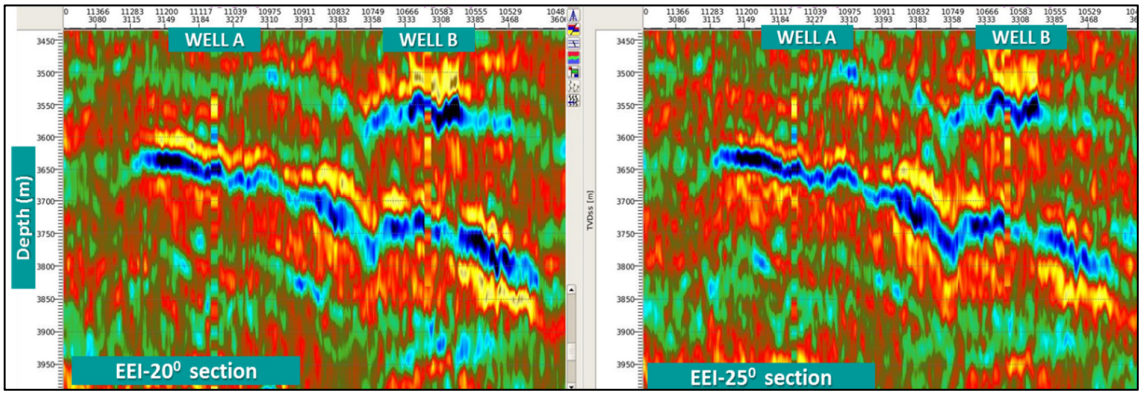

Figure-6 Band pass Inverted section of EEI (20) & EEI (25) shows good match with actual log. Gas sand and brine sand are very well delineated from the background.

Aquifer mapping in Deep water Miocene sand using Extended Elastic Impedance Attributes -A case study from Mahanadi Basin

Geocellular model and Reservoir Simulation

Object-based geocellular model was prepared to estimate in-place hydrocarbon volume and predict dynamic behavior of the reservoir. The reservoir facies and porosity variations were captured using logs as the hard constraint at both the wells and EEI impedance volume data was used to demarcate the channels. The sand facies observed above gas water contact in the well A is considered as gas sand and sand facies below it is considered as brine sand. Dynamic model was then prepared by integrating rock, fluid and well data to the static model. Extent of brine sand was captured by attaching analytical aquifer to the reservoir. The resultant model was used to predict the dynamic behavior of the reservoir.

Results

Extension of gas and brine sands were demarcated effectively in EEI (200) and EEI (250) attributes Extracted on top of reservoirs as shown in Figure-7. The dynamic model with analytical aquifer replicating the brine sand helped to understand the aquifer behavior. A case without analytical aquifer (Case-1) was compared to another case with analytical aquifer (Case-2). Figure-8 shows that the water influx to the eastern and southern part of the reservoir is much faster in Case-2 than expected from Case-1.

Study of water movement for Case-2 suggested further scope for optimizing the development well locations. Accordingly, sensitivity analysis was carried out on the dynamic model with analytical aquifer (Case-2) to optimize the well locations. The Figure-8 shows one of the well location selected on the basis of the sensitivity study. The new development well location resulted in delayed water breakthrough in the well thereby improving the well performance as shown in Figure-8.

Conclusion

Petro physical property volumes are effectively generated in terms of impedances using EEI inversion. Aquifer extension was mapped and used in geocellular model and reservoir simulation. This approach helped in optimizing the development wells by mitigating the risk of early water influx thus adding confidence to the production prediction.

Acknowledgement

This technical paper is part of the project work carried out at RIL. The authors are thankful to RIL authority for permitting to publish the work as technical paper. The authors express their gratitude to Shri Pranaya Sangvai (Head Mahanadi Business Unit) and Shri Bhagaban Das (Head Reservoir Characterization Group) for giving opportunity to carry out this project. The authors also want to thank the concerned team members for providing technical input during the execution of the project.

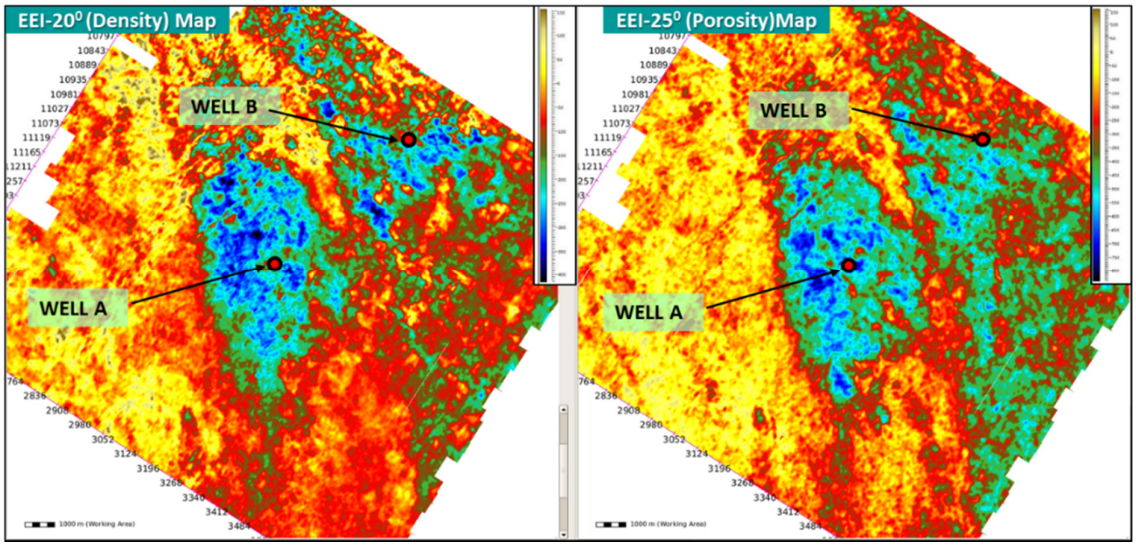

Figure-7 Gas sand and brine sand are well captured in EEI (20) & EEI (25) attributes maps corresponding to density and porosity.

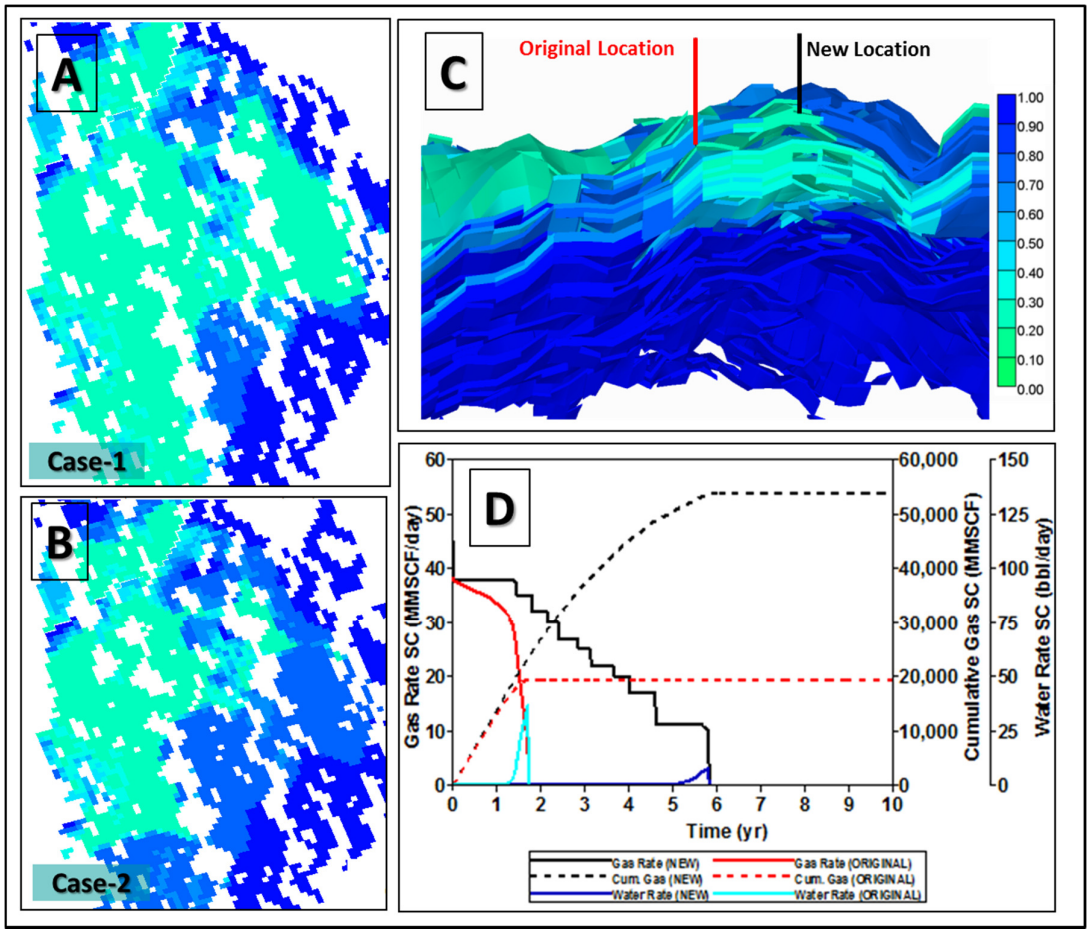

Figure-8 Comparison of aquifer influx for no aquifer case (A) vis-à-vis analytical aquifer case (B). New well location (C) based on water movement in dynamic model. Comparison of well performance (D) of New well vis-à-vis Original well for aquifer sensitivity performed on analytical aquifer model.

References

- David N. Whitcombe, Patrick A. Connolly, Roger L. Reagan, and Terry C. Redshaw (2002). ”Extended elastic impedance for fluid and lithology prediction.” Extended elastic impedance for fluid and lithology prediction 67, SPECIAL SECTION—SEISMIC SIGNATURES OF FLUID TRANSPORT, 63-67.doi: 10.1190/1.1451337
- D. N. Whitcombe, M. Dyce, C. J. S. McKenzie, and H. Hoeber (2004) Stabilizing the AVO gradient. SEG Technical Program Expanded Abstracts 2004: pp. 232-235.doi: 10.1190/1.1839698